

## A microwave active filter for nanosatellite's receiver front-ends at S-band

Linh Ta Phuong<sup>1</sup>, Bernard Journet<sup>2</sup>, Duong Bach Gia<sup>3</sup>

<sup>1</sup>Vietnam Space Center, Ministry of Science and Technology, Vietnam

<sup>2</sup>Quantum and Molecular Photonics Laboratory, ENS Paris-Saclay, France

<sup>3</sup>VNU University of Engineering and Technology, Hanoi, Vietnam

---

### Article Info

#### Article history:

Received May 30, 2018

Revised Sep 17, 2018

Accepted Nov 3, 2018

#### Keywords:

Coupled line bandpass filter

Microwave active filter

Nanosatellite

Receiver fronts end

Wideband low noise amplifier

---

### ABSTRACT

In satellite technology, the communication between space segment and ground segment plays a vital role in the success of the mission. This paper is targeted at study, design and fabrication of a microwave active filter for the receiver front-ends using coupled line filter structure, which can be applied to the nanosatellite's communication subsystem. The whole active filter module is a combination of a microstrip bandpass filter and a preceding two-stage wideband low noise amplifier using FET devices. The proposed module operates in the frequency range of 2 - 2.4 GHz, which can be divided to 10 frequency slots of about 40 MHz for each. These frequency slots will be used for the S-band multi-frequency receiving function of the ground station, as well as the nanosatellite. The simulated and measured results of this active filter configuration are presented.

Copyright © 2019 Institute of Advanced Engineering and Science.  
All rights reserved.

---

### Corresponding Author:

Bernard Journet,

Quantum and Molecular Photonics Laboratory, ENS Paris-Saclay,

61 Avenue du Président Wilson, 94230 Cachan, France.

Email: bernard.journet@ens-cachan.fr

---

## 1. INTRODUCTION

Small satellites have been widely applied in communications satellite in recent years. In this section, nanosatellite is being regarded as a proper choice for satellite communication in developing countries, because of its low fabrication budget, ability of integrating numerous in a single launch vehicle, and the possible of arranging in constellation for in-situ operation. The wet mass of a typical nanosatellite lies between 1 and 10 kg, and its dimensions seldomly exceed 30 cm.

The performance of a receiver module mainly depends on the bandpass filter (BPF) and low noise amplifier (LNA) units. Without these parts, the receiver is unable to distinguish the weak receiving signal from the noise. Consequently, the bit error rate (BER) will increase drastically and certainly lower the quality of the receiving message. Therefore, designing good filtering and low noise amplifying modules are prime requirements of a successful satellite communication mission.

In the filter region, there are four major parameters govern the dissipation loss level of a bandpass filter: The filter type, the order of the filter, the unloaded Q-factor of the filter elements and the bandwidth. Universally, all passive bandpass filtering structures encounter a problem of compromising between insertion loss and bandwidth, especially at radiofrequency. For details, the product of these two parameters is a constant [1], a narrower bandpass filter means higher degree of insertion loss. Furthermore, in microwave frequencies, it is really a challenge to construct a high-performance filter with passive elements only, because of the detrimental effects of the parasitic elements. Electronics researchers have taken much efforts to deal with these problems for decades, and thanks to the development of the semiconductor technology, a very promising solution for this limitation is established: Using field effect transistors (FET) as active elements to compensate the insertion loss while maintaining the bandwidth quality of the filter.

The module consists of the microwave filter and the active element, which is the LNA in our case, is called Microwave Active Filter (MAF). Figure 1 shows the block diagram of a typical receiver including the MAF unit:

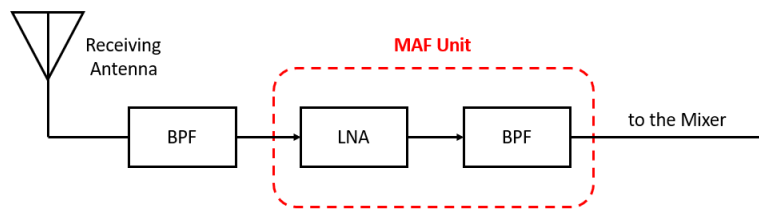


Figure 1. The receiver with MAF

In the above figure, the receiving signal first goes through a bandpass filter, which lies outside the MAF unit, for a primary filtering process. This filter is necessary because the raw receiving signal is very noisy and contains some amplitude perturbation superimposing components, which can lead to an overload in the LNA. After being filtered, the signal enters the MAF unit and being amplified to a desired amplitude level by the LNA, then goes through the BPF of the MAF for a smooth filtering process. Subsequently, at the input of the mixer of the IF stage, we have a low noise, well-amplified signal at the desired RF band.

There are previous works related to MAF. In their electronics letter, Chang and Itoh (1989) [2] published a narrowband MAF using microstrip distributed elements, based on the coupled negative resistance method. R.Gracia and J.Alonso [3] demonstrated a High-selective microwave active bandpass filter using transmission line interference sections with a passive filter precedes an active interference stage. Though these topologies showed good results at S-band, it is fairly difficult to put them into application of a high order microstrip filter for a nanosatellite receiver because of its complexity. Cheng *et al.* (2000) published a novel way to increase the linearity and noise performance of microwave active bandpass filters using the negative-resistance compensated topology [4]. A structure includes an LNA and a bandpass filter called as the Selective RF Low Noise Amplifier, which can be used in FM broadcast band (88 – 108 MHz), is introduced by Lee and Lu [5]. An active 8-path filter with a preceding LNA for software-defined radio (SDR) transceivers, in which the center frequency can be tuned from 100 MHz to 2 GHz is presented by Behmanesh and Atarodi [6]. L.Pantoli *et al.* [7] illustrated a tunable active filter topology for microwave applications. However, these mentioned works used lumped filter elements and can only be effectively applied for the frequency range of below 2 GHz, it is fairly difficult to apply these designs in the frequency range of over 2 GHz when taking the dissipation loss and parasitic effects into account, especially when integrating them in a satellite that operating in a harsh environment. Mariem and Nabih [8] designed an active bandpass filter based on operational transconductor amplifiers using simple CMOS current mirrors, this filter structure has very good return loss (S11) and insertion loss (S21) responses and can also be tuned to operate at the frequency range of about 2 GHz by modifying the value of the grounded capacitor and inductor of this topology. However, the passband bandwidth is very narrow (about 15 MHz) and it might not suitable for our mission. Y.Hao *et al.* (2008) mentioned a MAF solution for satellite's receiver front-ends by placing a bandpass filter in front of the LNA to choose the desired frequency band and reduce the noise, which is very similar to our method [9]. However, the authors only demonstrated the filter design process and optimized the results by using Advance Design System (ADS) but ignore the role of the LNA. Furthermore, the filter design of the authors seemed not to be practical enough to apply to a real satellite front-end receiver.

Our designing purpose is to obtain the best trade-off between operation frequency, total efficiency of the system, and simplicity. The key features of the proposed MAF are listed below:

- a) Has a relative high gain and low noise figure.
- b) Provides least distortion to the frequency response.
- c) Has the ability of tuning frequency in a wide range at S-band. In our case, the entire range is from 2 GHz to 2.4 GHz with 10 internal frequency slots.
- d) Compact enough to be integrated to the receiver system in either space segment (nanosatellites) or earth segment (small ground stations).

**2. DESIGN AND SIMULATION OF THE COUPLED LINE BANDPASS FILTER**

The microstrip coupled line bandpass filter is widely used in radiofrequency, because of its equilibrium between performance, simplicity and manufacturing expenses. Similar to a single microstrip line, a coupled microstrip line is a quasi-TEM mode system with no cut-off frequency. For microwave frequency, the filtering topology using microstrip distributed elements have many benefits over the lumped elements topology, such as reducing the parasitic effects, easier to produce, and offering much smaller area and profile.

In the microstrip coupled lines, there are two different modes of field distribution, namely the odd-mode and even-mode, which can be physically explained by the positions of the relative polarities of voltages along the transmission lines. Consequently, it leads to the two characteristic impedances called the odd-mode characteristic impedance ( $Z_{0o}$ ) and even-mode characteristic impedance ( $Z_{0e}$ ), which are the two primary parameters in the design procedure [10]. Figure 2 demonstrates the field distribution of these two modes:

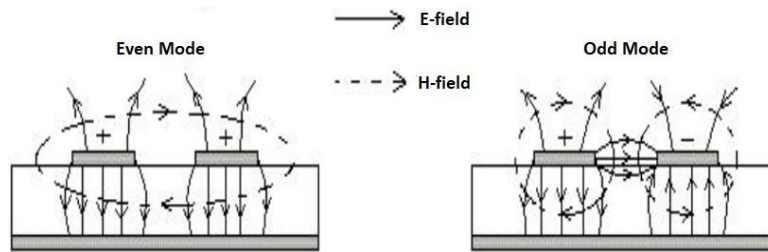


Figure 2. The field distribution over odd and even modes of the coupled lines [10]

A half-wavelength parallel coupled line microstrip bandpass filter is a structure included coupled lines which are paralleled in pairs along half of their lengths. Once appropriately spacing the resonator elements, we have a good coupling, thus providing the desired bandwidth. The spacing parameters (or gaps) are denoted by  $S$ . Along with the gap, there are other governing parameters, namely length ( $l$ ), width ( $W$ ) and characteristic admittance ( $Y_0$ ), which is just the inverse of the characteristic impedance,  $Z_0$ , of the connecting line. The filter structure is demonstrated in Figure 3:

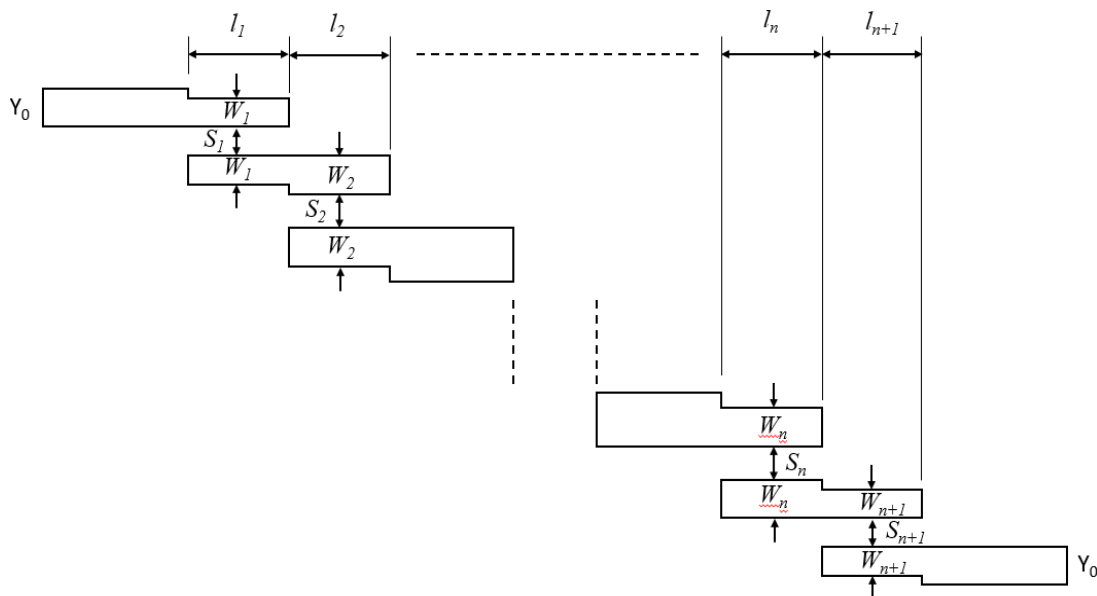


Figure 3. The structure of the microstrip parallel coupled line bandpass filter (redrawn from [11])

The equations are used to design the filter:

$$J_{0,1}Z_0 = \sqrt{\frac{\pi.FBW}{2g_0g_1}} \tag{1}$$

$$J_{j,j+1}Z_0 = \frac{\pi.FBW}{2\sqrt{g_j g_{j+1}}} \text{ for } j=1 \text{ to } n-1 \tag{2}$$

$$J_{n,n+1}Z_0 = \sqrt{\frac{\pi.FBW}{2g_n g_{n+1}}} \tag{3}$$

Where  $g_0, g_1, \dots, g_n$  are element values, in our case:  $g_0 = g_4 = 1, g_1 = g_3 = 1.5963, g_2 = 1.0967$  [12]. FBW is the filter's fractional bandwidth.  $Z_0$  is the characteristic impedance of the line, as explained before and  $J$  (with subscribes) is the characteristic admittances of the inverters. Based on the above equations, we can calculate the characteristic impedances of the odd and even modes of the parallel coupled line microstrip bandpass filter as follows:

$$(Z_{0,o})_{j,j+1} = Z_0(1 - J_{j,j+1}Z_0 + (J_{j,j+1}Z_0)^2) \tag{4}$$

$$(Z_{0,e})_{j,j+1} = Z_0(1 + J_{j,j+1}Z_0 + (J_{j,j+1}Z_0)^2) \tag{5}$$

In this design, we chose the 3rd order filter with 2 pairs of symmetric filter elements. The calculated values (in Ohms) of the characteristic impedances are shown in Table 1.

Table 1. Odd and even Impedances Values Calculated from the Impedance Inverter Parameters

Filter stage	Odd mode impedance ( $Z_{0o}$ )	Even mode impedance ( $Z_{0e}$ )
0	51.68	79.57
1	46.47	89.76

The material used for the filter structure is Rogers FR4, which has the following characteristics: Relative dielectric constant: 4.34, loss tangent: 0.0025, dielectric height: 1.6 mm, conductor thickness: 0.035 mm, roughness: 0.0095. The simulated results in Decibel of the input reflection coefficient (S11) and insertion loss (S21) have been done by the Advanced Design System (ADS) 2014, provided by Agilent. The schematic design and simulated results are illustrated in Figure 4 and Figure 5, respectively.

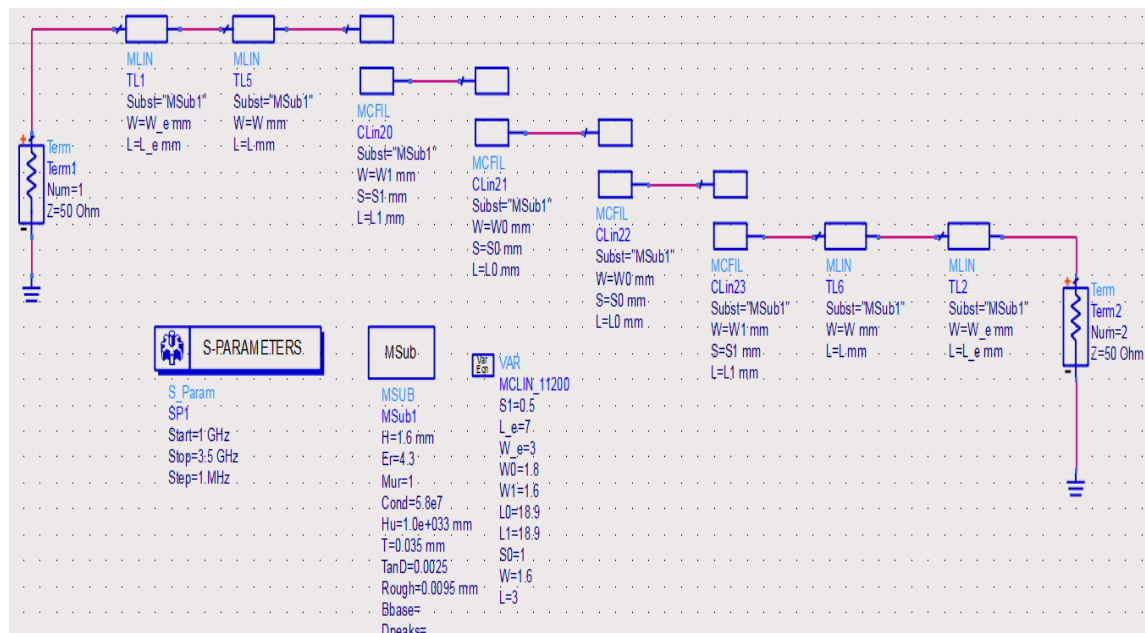


Figure 4. The schematic of the simulated parallel coupled line microstrip bandpass filter

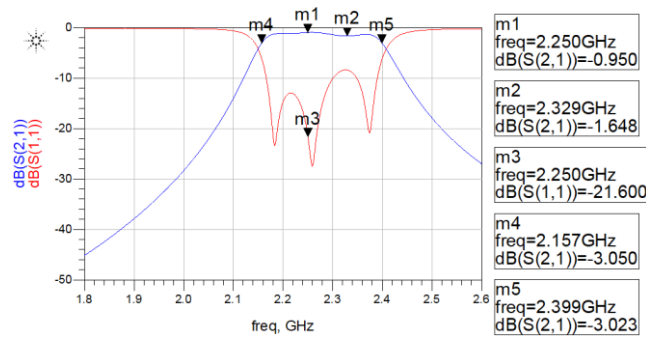


Figure 5. The simulated results of S11 and S21 using FR4 substrate

The results are simulated based on the formulae from (1) to (5), without abusing the Optimization Tool of the ADS software, because this type of tool may leads to nonreproducible and non-systematic solutions [13]. As can be seen in Figure 5, the insertion loss (S21) and return loss (S11) is around 0.95 dB and 21.6 dB at 2.25 GHz, respectively. Furthermore, the ripple in the whole passband is roundly 0.7 dB and the 3-dB bandwidth is approximately 250 MHz. This result is not suitable to apply to the total frequency range of 400 MHz of our desired receiver front-end, thus we must add an LNA module to widen the bandwidth while maintaining the above figure of merit of the filter.

### 3. DESIGN AND SIMULATION OF THE WIDEBAND LOW NOISE AMPLIFIER

The low noise amplifier plays a vital role in satellite's receiver, its main function is to amplify the weak received signal which goes through the satellite's antenna terminal. Along with the operational frequency and bandwidth, the LNA design is governed by the following parameters:

- Noise figure: The noise figure of the LNA is directly added to that of the receiver, so it should be small enough in order to avoid harmful effect to the total noise figure of the receiver.
- Gain: The gain of LNA should be large enough in order to reduce the noise contribution of the subsequent stages to minimum [14].
- Input return loss: This parameter shows the performance of the impedance matching between the input of the LNA and the output of the preceding equipment (i.e the antenna).

In most cases, the LNA should be placed as close as possible to the output of the receiving antenna to minimize the distant loss and thermal noise caused by the connecting cables. From another point of view, the LNA can also act as an active element of a filtering system when positioning it prior to a filter. This leads to some considerable benefits to the signal such as noise compensating, gain boosting and the ability of tuning the peaked gain for frequency selection.

In our case, an additional requirement is to maintain an acceptable gain in the frequency range of 2-2.45 GHz. In order to obtain the best compromise between the three above parameters, a two-stage LNA configuration is being considered, in which, the first stage is to optimize the signal's bandwidth as well as noise figure and the second stage is to rise the overall gain. The transistor type used in this LNA topology is SPF-2086, which is fabricated pHEMT GaAs FET technology with high gain, low noise figure and has an operating frequency from 0.1 GHz up to 12 GHz. Figure 6 shows the block diagram of the desired 2-stage LNA:

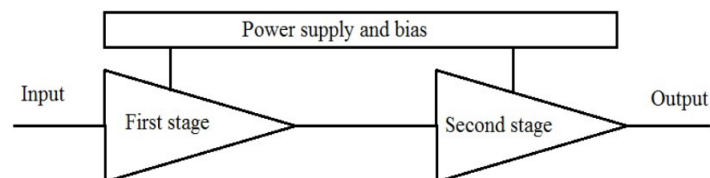


Figure 6. Block diagram of the 2-stage cascaded LNA [15]

The LNA network can only work efficiently once being impedance matched properly in both of its input and output. The purpose of impedance matching is to maximize the transferred power from the source

to the load and minimized the reflected power from the load to the source, thus optimize the voltage standing wave ratio (VSWR). The figure below demonstrates a typical matching system, which includes input and output matching networks for a single stage of our LNA:

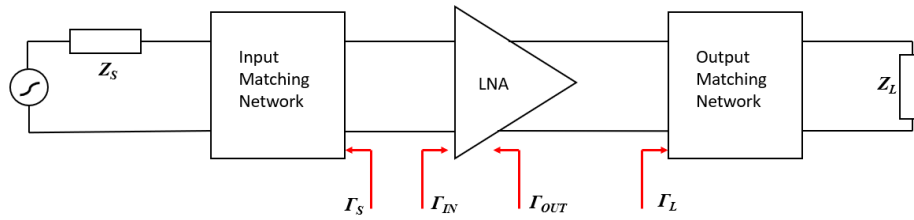


Figure 7. The diagram of impedance matching networks of the single stage of the LNA

In Figure 7,  $Z_S$  needs to be matched with  $Z_L$ , and these parameters both equal 50 Ohms, which is the characteristics impedance ( $Z_0$ ) of the transmission lines. In order to reach this, the values of the reflection coefficients of the input and output matching networks, namely  $\Gamma_S$  and  $\Gamma_L$ , need to be equalized to the corresponding reflection coefficients of the input and output,  $\Gamma_{IN}$  and  $\Gamma_{OUT}$ , of the LNA. Once the input and output of the LNA are both being matched, we can calculate the available power gain of the LNA, which is the ratio of the power available from the amplifier to the power available from the source [16].

The proposed LNA has the same structure as shown in Figure 8, with the desired bandwidth of 400 MHz and the operation center frequency of 2.3 GHz. The figure below is the schematic diagram of the 2-stage wideband LNA, using the same FR4 substrate as that of the previous coupled line BPF.

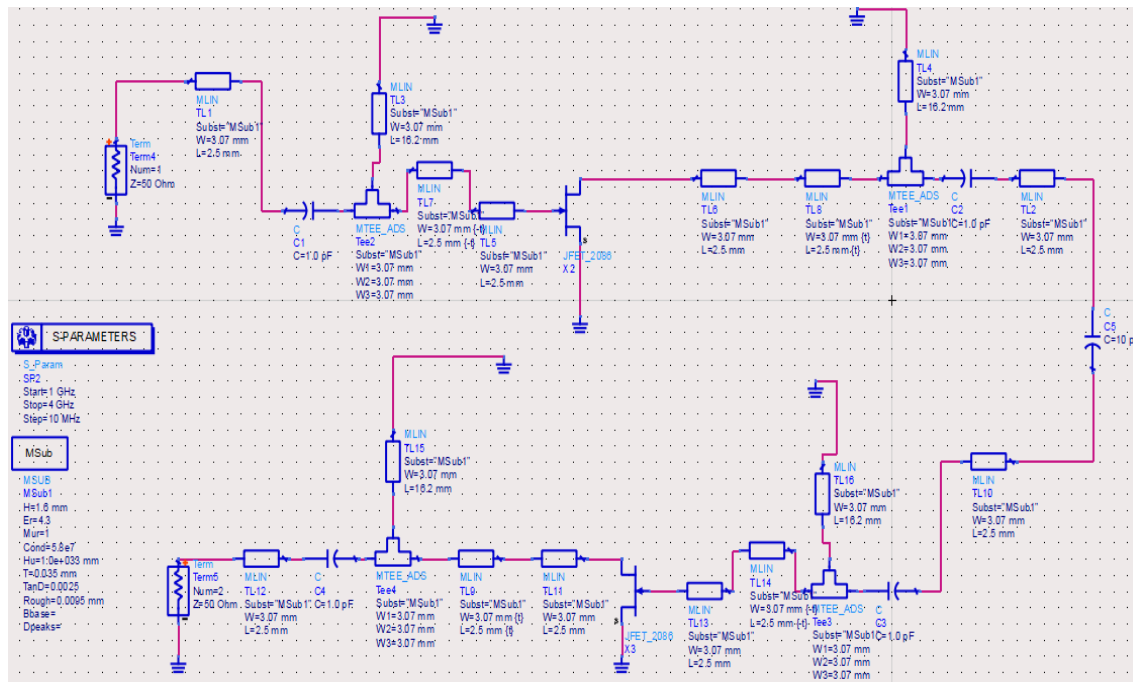


Figure 8. Schematic diagram of the 2-stage cascaded LNA

As can be seen in the above figure, the two stages are identical to each other. A 10-pF capacitor has been placed between the two stages in order to reduce the parasitic effect. The impedance matching technique used here is the combination of general and quarter-wave transmission lines. The quarterwave transformers are TL3, TL4, TL15 and TL16, respectively. The center frequencies of both stages are 2.3 GHz. The typical power supply of the SPF-2086 transistors are 5 V/50 mA and the biasing point is reached at -0.5 V. Figure 9 displays the simulated gain and input reflection coefficient of the 2-stage LNA:

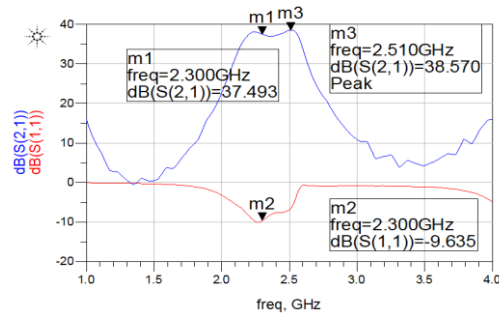


Figure 9. The simulated result of the 2-stage wideband LNA

It is clearly seen that in Figure 9, the overall power gain ( $S_{21}$ ) of the desired LNA is greater than 35 dB at the frequency range of 2.15 – 2.58 GHz, the maximum gain of 38.57 dB is obtained at 2.51 GHz. The input reflection coefficient,  $S_{11}$ , is approximately -9.6 dB at the desired frequency, which lies in the tolerance range.

#### 4. MEASURED RESULTS

The whole MAF circuit was successfully designed and fabricated in our laboratory based on the ADS package and the LKPF ProtoMat C40 machine. The testing results of the filter without connecting to the LNA are measured on the Vector Network Analyzer 37369D - Anritsu technology with the linearity range up to 40 GHz. Figure 10 and Figure 11 show the experimental results of the coupled line microstrip bandpass filter without LNA.



Figure 10. The measured  $S_{21}$  of the parallel coupled line microstrip bandpass filter



Figure 11. The measured  $S_{11}$  of the parallel coupled line microstrip bandpass filter

As can be seen in the above figures, the experimental results are well matched to the simulated results showed in Figure 5, the insertion loss peaked at around 2.25 GHz. The degrade of the  $S_{21}$  of the fabricated filter in Figure 10 is caused by cables and connectors' loss, this value is approximately 2.3 dB. Figure 12 shows the measured result of the MAF system, with the measured frequency ranged from 1.9 GHz

to 2.5 GHz. The measure was done by picking the amplitude values of the receiving signal over the measured frequency range with the frequency step of 2.5 MHz, corresponds to 240 points over the whole frequency span.

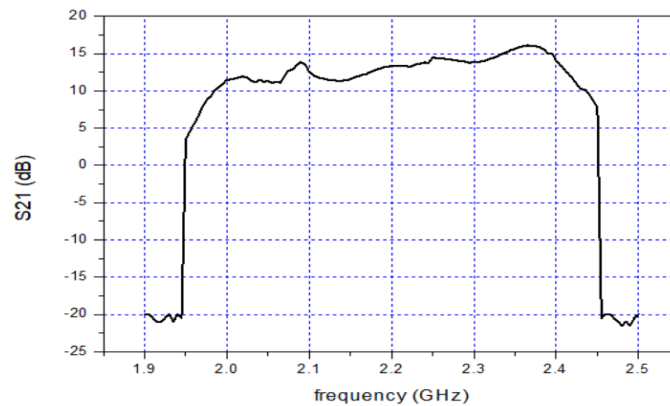


Figure 12. The measured  $S_{21}$  of the whole microwave active filter

In Figure 12, the operation frequency range is between 2 GHz and 2.4 GHz, which corresponds to a bandwidth of 400 MHz. The highest gain value is 16.1 dB at around 2.36 GHz and the gain values around the center frequency of the bandpass filter are approximately 14 dB. The actual peaked gain without respect to the cables and connector attenuations is about 20 dB. The fluctuation of the gain range is roundly 5 dB, however, it can be compensated by the S-band receiver's automatic gain control (AGC). A noticeable trait of the above gain diagram is that the values fall rapidly outside the desired range, for details, from 10 dB at 1.98 GHz to -20 dB at 1.95 GHz and from 10 dB at 2.43 GHz to -20 dB at 2.45 GHz. This leads to a good frequency selective characteristic of our MAF. However, the most important point, which is also the main goal of our design is that the MAF has the ability of flexibly tuning the frequencies over the whole operational frequency bandwidth. As can be seen in Figure 12, the  $S_{21}$  of the 2 GHz – 2.4 GHz range considerably fluctuates from 11 dB to 16 dB. However, when dividing this to 10 internal frequency slots of 40 MHz we have flattened sub-ranges, in which, the vibrations of  $S_{21}$  is less than 1 dB. These local frequency spans allow the front-end receiver to perform multi-frequency receiving in the whole desired range. This can be done by integrating the receiver to a frequency switching circuit. Furthermore, the frequency slots can be further increased when combining the MAF with a phase-locked loop (PLL) frequency synthesizer unit in order to do the flexible stepped tuning [17]. It provides undeniable advantages to the multi-frequency satellite communication.

## 5. CONCLUSION

This paper introduced about a microwave active filter consists of a coupled line microstrip bandpass filter and a wideband low noise amplifier. The simulated and measured results are being presented and it proved good agreement between simulation and practice. The MAF is successfully designed and operated at S-band, and it can be applied to nanosatellite's receiver fronts-end at both space and ground segments. The operation range of the proposed MAF is 2-2.4 GHz and the highest gain value is around 20 dB. The MAF allows good stepped frequency tuning at S-band and it proves considerable benefits in comparison to general passive filter systems, such as: Provides considerable high gain signal at the operating band, better frequency response and noise compensating for the filter, and still compact enough to integrate to the nanosatellite's receivers. Based on the requirement of the communication satellite missions, the flatness and frequency response of the operation band can be further improved when increasing the order of the filter, this can be used for applications that required smooth frequency tuning.

## REFERENCES

- [1] B.Y. Kapilevich, "Variety of Approaches to Designing Microwave Active Filters," *Microwave Conference, 27th European*, 1997; 1: 397-408.

- [2] C.Y. Chang and T. Itoh, "Narrowband Planar Microwave Active Filter," *Electronics Letters* 31st, Aug. 1989; 25: 1128-1129.
- [3] R. Gracia and J. Alonso, "High-selective microwave active bandpass filter using transmission line interference sections," *34th European Microwave Conference, Amsterdam, The Netherlands, 2004*; 721-724.
- [4] K.M. Cheng, Hil-Ye Chan, Kim-Fung Yip, "Optimization of Linearity and Noise Performance of Microwave Active Bandpass Filters," *Asia-Pacific Microwave Conference. Proceedings* (Cat. No.00TH8522), Sydney, NSW, Australia, 2000; 197-200.
- [5] K.K. Lee and Y. Lu, "A Selective RF Low Noise Amplifier," in *Radio Project, Department of Electrical and Information Technology*, Lund University; 2009.
- [6] B. Behmanesh and S.M. Atarodi, "Active Eight-Path Filter and LNA with Wide Channel Bandwidth and Center Frequency Tunability," *IEEE Transactions on Microwave Theory and Techniques*, Nov. 2017; 65(11): 4715-4723.
- [7] L. Pantoli, V. Stornelli, G. Leuzzi, "Tunable Active Filters for RF and Microwave Applications," *Journal of Circuits, Systems, and Computers*, 2014; 23(6): 1450088.
- [8] J. Mariem and Pr.Ou. Nabih, "Design of an OTA-based Microwave Active Filer," *International Conference on Wireless Technologies, Embedded and Intelligent Systems (WITS)*, Fez, Morocco 2017; 1-4.
- [9] Y. Hao, B. Zu, P. Huang, "An Optimal Microstrip Filter Design Method Based on Advanced Design System for Satellite Receiver," *IEEE International Conference on Mechatronics and Automation*, Takamatsu, Japan, 2008; 903-907.
- [10] A.R. Othman and C. Wasli, "2.4 GHz Microstrip Bandpass Filter," *The 1st International Conference on Engineering and ICT*, Melaka, Malaysia, 2007.
- [11] J.S. Hong, "Microstrip Filter for RF/Microwave Application," Second Edition, New York: John Wiley and Sons. 2011: 130-131.
- [12] D. M. Pozar, "Microwave Engineering," Third Edition, New York: John Wiley and Son. 2005: 370 - 421.
- [13] L. Billonnet, "Active Filters: Tools and Techniques for Active-filter Design," *Encyclopedia of RF and Microwave Engineering*. Sixth Volume, New York: John Wiley and Sons. 2015: 70-88.
- [14] B. Razavi, "RF Microelectronics," Second Edition, New Jersey: Prentice Hall Communications Engineering and Emerging Technologies Series. 2012: 255-262.
- [15] T.V. Hoi and B.G. Duong, "Study and design of wide band low noise amplifier operating at C band," *VNU Journal of Mathematics – Physics*. 2013; 29(2): 16-24.
- [16] Abu Bakar Ibrahim, Ahmad Zamzuri Mohamad Ali, "Design of Microwave LNA Based on Ladder Matching Networks for WiMAX Applications," *International Journal of Electrical and Computer Engineering (IJECE)*. 2016; 6(4): 1717-1724.
- [17] The Anh Nguyen Dinh, Huy Le Xuan, Tuan Anh Vu, Duong Bach Gia, "A Status Data Transmitting System for Vessel Monitoring," *International Journal of Electrical and Computer Engineering (IJECE)*. 2018; 8(2): 917-925.

## BIOGRAPHIES OF AUTHORS



**Linh Ta Phuong** received the M.Sc. Degree in Electronics and Telecommunications Technology from University of Engineering and Technology, Vietnam National University in 2014 and M.Sc. Degree in Aerospace Engineering from Tohoku University in 2017. From 2015 up to now, he is a researcher in Vietnam National Space Center, Vietnam Academy of Science and Technology. His researches mainly focus on microwave engineering, communications in satellites, ground station and radio systems.

Email: [tplinh@vnsc.org.vn](mailto:tplinh@vnsc.org.vn)



**Linh Ta Phuong** received the M.Sc. Degree in Electronics and Telecommunications Technology from University of Engineering and Technology, Vietnam National University in 2014 and M.Sc. Degree in Aerospace Engineering from Tohoku University in 2017. From 2015 up to now, he is a researcher in Vietnam National Space Center, Vietnam Academy of Science and Technology. His researches mainly focus on microwave engineering, communications in satellites, ground station and radio systems.

Email: [tplinh@vnsc.org.vn](mailto:tplinh@vnsc.org.vn)



**Duong Bach Gia** was born in Ha Dong Dist., Hanoi, Vietnam in 1950. He received the B.S degree in radio physics in 1972 and the Ph.D. degree in wireless physics from University of Hanoi in 1988. From 1988 to 1990, he was a researcher assistant in Leningrad University, Russia. From 1991 to 2005, he was a researcher in academy of air force. He has been a lecturer and head of electronics and telecommunications center, University of Engineering and Technology, Vietnam National University since 2006. He was promoted to Associate Professor in 2009 and to Professor in 2016. His research focuses on RF analog signal processing, RF chip design, radar engineering and technology, automatic control.

Email: [duongbg@vnu.edu.vn](mailto:duongbg@vnu.edu.vn)